Letter

Exactly solvable model of light-scattering errors in quantum simulations with metastable trapped-ion qubits

Phillip C. Lotshaw [1,*] Brian C. Sawyer [2] Creston D. Herold [2] and Gilles Buchs [1]
[1]*Quantum Information Science Section, Oak Ridge National Laboratory, Oak Ridge, Tennessee 37381, USA*
[2]*Georgia Tech Research Institute, Atlanta, Georgia 30332, USA*

(Received 16 July 2024; accepted 27 August 2024; published 9 September 2024)

We analytically solve a model for light scattering in Ising dynamics of metastable atomic qubits, generalizing the approach of Foss-Feig *et al.* [Phys. Rev. A **87**, 042101 (2013)] to include leakage outside the qubit manifold. We analyze the influence of these fundamental errors in simulations of proposed experiments with metastable levels of $^{40}Ca^{+}$ ions in a Penning trap. We find that "effective magnetic fields" generated by leaked qubits have significant impacts on spin-spin correlation functions for Greenberger-Horne-Zeilinger state preparation or for quantum simulations with strong coupling, while spin squeezing uses a much weaker coupling and is largely insensitive to the simulated leakage errors, even with a few hundred ions. Our theory and results are expected to be useful in modeling a variety of metastable qubit experiments in the future.

DOI: 10.1103/PhysRevA.110.L030803

Introduction. Metastable atomic qubits offer multiple advantages over more traditional ground or optical qubit encodings. Their use expands the range of available wavelengths for qubit control, notably increasing the wavelength of optical controls relative to those of ground-state qubits [1] and a practical advantage is the availability of high-power near-infrared lasers for metastable qubit operations. However, metastable qubits also have distinct fundamental errors due to photon-scattering pathways that are not present in ground-state encodings. To better understand these errors we solved a model of light scattering dynamics in metastable-qubit quantum simulations.

Our work builds on a previous analysis of Foss-Feig *et al.* [2], who analytically solved a model for nonequilibrium dynamics of an Ising interaction in which spontaneous photon scattering leads to fluctuating spins which mimic a noisy magnetic field. Their model gave a good account of decoherence in quantum simulations with $^{9}Be^{+}$ ions in the NIST Penning trap system, which has been used to demonstrate spin squeezing of hundreds of ions [3], out-of-time-order correlations in spin magnetization [4], and force sensing [5]. While scattering in $^{9}Be^{+}$ ground-level qubits remained confined to the qubit manifold, here we consider metastable qubits such as the $^{2}D_{5/2}$ levels of $^{40}Ca^{+}$ [6] depicted as $|0\rangle$ and $|1\rangle$ in Fig. 1(a). Light scattering from these qubit levels predominantly induces leakage to the ground state $|g\rangle$, which can be detected without disturbing the metastable qubit. Unlike scattering errors within the qubit manifold, detecting these leakage errors has benefits for quantum error correction schemes utilizing "erasure conversion" [7,8]. Quantum simulation accuracy can also be improved by detecting and discarding results with leakage, at the cost of additional sampling overhead, as we quantify below.

Here we analytically solve a model for decoherent Ising dynamics with light scattering and leakage, with generic metastable qubits as illustrated in Fig. 1(b). We examine the influence of light scattering errors in proposed experiments with $^{40}Ca^{+}$ [Fig. 1(a)], where we include an additional analytic treatment of a spin-echo sequence. We find differences in leakage error sensitivity for strongly coupled quantum spin dynamics and Greenberger-Horne-Zeilinger (GHZ) state preparation, in contrast to spin squeezing and a simple single-layer benchmarking implementation of the quantum approximate optimization algorithm (QAOA). Our results are expected to be useful in analyzing future experiments with metastable trapped-ion qubits.

Light shift interaction. Applying two off-resonant laser beams to N trapped ions generates an instantaneous optical dipole force Hamiltonian

$$H(t) = \sum_{i=1}^{N} F_0 \cos(\mu t)\hat{z}_i \sigma_i^z, \tag{1}$$

where F_0 is the force amplitude and μ is the laser beatnote angular frequency [3,9]. Here σ_i^z represents the Stark shift to the electronic energy levels of ion i, coupled to the vibrational states through the position operator $\hat{z}_i$. This "spin-dependent force" causes vibrational modes to traverse loops in phase space with periods $T_m = 2\pi/\delta_m$, where $\delta_m = \mu - \omega_m$ is the detuning from resonance with respect to mode m, with angular frequency ω_m [9]. When a mode returns to its origin it becomes disentangled from the electronic levels, leaving a residual geometric phase which is exploited for quantum information processing. These phases yield an effective Ising evolution $\exp(-i\mathcal{H}t)$ after integrating (1) in the Lamb-Dicke approximation and using a spin-echo sequence to cancel undesired "longitudinal field" terms $\sim\sigma_i^z$ [9,10], where

$$\mathcal{H} = \frac{1}{N}\sum_{i<j} J_{ij}\sigma_i^z\sigma_j^z, \tag{2}$$

*Contact author: Lotshawpc@ornl.gov

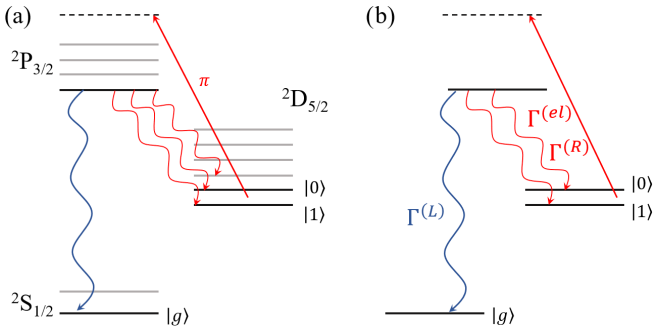

FIG. 1. (a) Partial electronic energy-level diagram of $^{40}Ca^+$ including metastable qubit levels $|0\rangle$ and $|1\rangle$ in the $^2D_{5/2}$ manifold. A π-polarized far-detuned laser beam (straight arrow) generates ac Stark shifts of the qubit levels through their interaction with the indicated $^2P_{3/2}$ level (black line). Off-resonant light scattering generates errors through allowed decay pathways (wavy lines). (b) Simplified level diagram used for analytic calculations with generic metastable qubits. The $\Gamma^{(R)}$, $\Gamma^{(el)}$, and $\Gamma^{(L)}$ are rates of Raman scattering in the qubit manifold, elastic scattering, and leakage to the ground state $|g\rangle$, respectively.

with

$$J_{ij} = N\Omega_i\Omega_j \sum_m \frac{\eta_{i,m}\eta_{j,m}\omega_m}{\mu^2 - \omega_m^2}, \tag{3}$$

where $\eta_{i,m}$ is a Lamb-Dicke parameter.

Ising dynamics with light scattering and leakage. Uys *et al.* [11] derived a Lindbladian master equation that accurately described single-ion light-scattering errors in $^9Be^+$. Foss-Feig *et al.* [2,12] applied the same error model to the effective Ising evolution (2) and, remarkably, obtained an analytic formula that successfully described decoherence in spin-squeezing experiments with hundreds of ions [3]. We generalize this approach to include leakage [Fig. 1(b)].

We consider an experimentally relevant [13–15] initial state $|\psi_0\rangle = |+\rangle^{\otimes N}$ evolving under the Lindbladian master equation [2,11]

$$\dot{\rho} = -i(\mathcal{H}_{\text{eff}}\rho - \rho\mathcal{H}_{\text{eff}}^\dagger) + \mathcal{D}(\rho), \tag{4}$$

where the effective non-Hermitian Hamiltonian $\mathcal{H}_{\text{eff}}$ and dissipator $\mathcal{D}(\rho)$ are

$$\mathcal{H}_{\text{eff}} = \mathcal{H} - i\sum_{\alpha,j} \mathcal{J}_j^{(\alpha)\dagger}\mathcal{J}_j^{(\alpha)}, \quad \mathcal{D}(\rho) = 2\sum_{\alpha,j} \mathcal{J}_j^{(\alpha)}\rho\mathcal{J}_j^{(\alpha)\dagger}. \tag{5}$$

Jump operators $\mathcal{J}_j^{(\alpha)}$ are included for each type of scattering event indicated in Fig. 1(b), including elastic scattering with $\mathcal{J}_j^{(el)} = \sqrt{\Gamma^{(el)}/8}\sigma_j^z$ as well as inelastic scattering with $\mathcal{J}_j^{(a\to b)} = \sqrt{\Gamma^{(a\to b)}/2}\,|b_j\rangle\langle a_j|$ for $a_j \in \{0,1\}$, $b_j \in \{0,1,g\}$ with $b_j \neq a_j$. The latter transitions include Raman scattering $|0\rangle \leftrightarrow |1\rangle$ within the qubit manifold, with the single-ion Raman decoherence rate $\Gamma^{(R)} = (\Gamma^{(0\to1)} + \Gamma^{(1\to0)})/2$, and leakage scattering to $|g\rangle$, with the single-ion leakage decoherence rate $\Gamma^{(L)} = (\Gamma^{(0\to g)} + \Gamma^{(1\to g)})/2$. The total single-ion decoherence rate is $\Gamma = \Gamma^{(L)} + \Gamma^{(R)} + \Gamma^{(el)}/2$.

We compute exact dynamics of (4) using the "quantum trajectories" approach [2,12,16]. The basic idea is to organize the evolution (4) into pure-state "trajectories" which are easier to analyze and are summed to produce the exact time-dependent state. The first term in (4) generates ideal evolution, with probability less than one. The second term $\mathcal{D}(\rho)$ produces quantum jumps under light scattering.

A key insight from Ref. [2] is that if a jump operator such as $\mathcal{J}_i^{(0\to1)} \sim |1_i\rangle\langle 0_i|$ is applied to an otherwise ideal state $|\psi\rangle$ at time t_i, this will generate a transition $|0_i\rangle \to |1_i\rangle$ and remove any part of the wave function that was in $|1_i\rangle$ before the jump occurred. Hence it will be as if the ion began in the state $|0_i\rangle$, which is an eigenstate of σ_i^z in the Ising interaction (2). Replacing σ_i^z with the corresponding eigenvalue leads to an "effective magnetic field" $N^{-1}\sum_{j\neq i} J_{ij}\sigma_i^z$ for time $t < t_i$ (for the state $|0_i\rangle$) and $-N^{-1}\sum_{j\neq i} J_{ij}\sigma_i^z$ for $t \geqslant t_i$ (after scattering to $|1_i\rangle$); note that we are using a convention in which $|1_i\rangle$ has lower energy than $|0_i\rangle$; see Fig. 1. In the case of multiple scattering events, the effective field strength depends on the difference in times $t_0 - t_1$ that the ion spends in $|0_i\rangle$ and $|1_i\rangle$. This idea was used previously to derive exact correlation functions including all possible Raman scattering processes within the qubit manifold [2]. The same idea remains essential in our treatment of leakage, which generates an effective field that "turns off" when an ion scatters to $|g_i\rangle$.

From (4) we derived a complete set of time-dependent operator expectation values $\langle\boldsymbol{\sigma}\rangle$, where $\boldsymbol{\sigma}$ is any product of raising $\sigma_i^+ = |0_i\rangle\langle 1_i|$ or lowering $\sigma_i^- = |1_i\rangle\langle 0_i|$ operators, or single-level projectors $\sigma_i^z = |z_i\rangle\langle z_i|$, acting on any arbitrary set of qubits. There is no coherence between the ground and qubit levels in our model, so operators describing these coherences (such as $|g_i\rangle\langle 0_i|$) have zero expectation. The $\boldsymbol{\sigma}$ form a basis for the relevant Liouville operator space; hence any operator O can be expressed as $O = \sum_{\boldsymbol{\sigma}} O_{\boldsymbol{\sigma}}\boldsymbol{\sigma}$ and its expectation can be computed as $\langle O\rangle = \sum_{\boldsymbol{\sigma}} O_{\boldsymbol{\sigma}}\langle\boldsymbol{\sigma}\rangle$. We can also compute $\rho(t)$ analytically. This generalizes the one- and two-spin analysis of Foss-Feig *et al.* [2] by extending to arbitrary many-body operators and by including leakage as a new error source. We verified these analytic results against direct numerical integrations of (4) using Simpson's method [17], with arbitrarily chosen nonuniform couplings and scattering rates, with up to four ions evolving for thousands of small time steps. We verified that our theory was correct to numerical precision for several physical quantities, including all matrix elements of the time evolving state $\rho(t)$. Detailed mathematical expressions and derivations are in Supplemental Material (SM) Secs. A and B [18].

As an example, we consider spin-spin correlation functions involving $\sigma_i^x = \sigma_i^+ + \sigma_i^-$ and $\sigma_j^y = -i(\sigma_i^+ - \sigma_j^-)$. To compute an m-body correlation function such as $\langle\prod_{j\in M}\sigma_j^x\rangle$, over a set of ions $M = \{j_1, j_2, \ldots, j_m\}$, we expand each σ_j^x in terms of σ_j^+ and σ_j^- to obtain a sum of 2^m expectation values $\langle\prod_{j\in M}\sigma_j^{\nu_j}\rangle$ with $\nu_j \in \{+,-\}$. For example, $\langle\sigma_i^x\sigma_j^x\rangle = \langle\sigma_i^+\sigma_j^+\rangle + \langle\sigma_i^+\sigma_j^-\rangle + \langle\sigma_i^-\sigma_i^+\rangle + \langle\sigma_i^-\sigma_j^-\rangle$, with similar expressions for $\langle\sigma_i^x\sigma_j^y\rangle$ and $\langle\sigma_i^y\sigma_j^y\rangle$. In SM we find that each of the $\langle\prod_{j\in M}\sigma_j^{\nu_j}\rangle$ can be expressed as

$$\left\langle\prod_{j\in M}\sigma_j^{\nu_j}\right\rangle = \frac{e^{-m\Gamma t}}{2^m}\prod_{i\notin M}\left[I\left(J_i^{(M,\boldsymbol{\nu})},t\right) + R\left(J_i^{(M,\boldsymbol{\nu})},t\right) + L\left(J_i^{(M,\boldsymbol{\nu})},t\right) + B\left(J_i^{(M,\boldsymbol{\nu})},t\right)\right], \tag{6}$$

where the functions I, R, L, B are defined below and $J_i^{(M,\nu)} = \sum_{j\in M} \nu_j J_{ij}$, with the notation $\nu_j J_{ij} = J_{ij}$ for $\nu_j = +$ and $\nu_j J_{ij} = -J_{ij}$ for $\nu_j = -$.

The prefactor $\exp(-m\Gamma t)$ is the product of single-ion decoherences for the m ions $j \in M$. Subsequent terms describe the influence of other ions through the Ising interaction, which is accounted for in terms of specific types of trajectories.

The first term

$$I\left(J_i^{(M,\nu)}, t\right) = e^{-\lambda t}\cos(st) \tag{7}$$

corresponds to ideal evolution, with inelastic relaxation rate $\lambda = (\Gamma^{(0\to1)} + \Gamma^{(0\to g)} + \Gamma^{(1\to0)} + \Gamma^{(1\to g)})/2$ and the effective damped oscillation frequency $s = s(J_i^{(M,\nu)}) = 2J_i^{(M,\nu)}/N + i\Delta$, which depends on the state-dependent scattering rate difference $\Delta = (\Gamma^{(0\to1)} + \Gamma^{(0\to g)} - \Gamma^{(1\to0)} - \Gamma^{(1\to g)})/2$.

The second term

$$R\left(J_i^{(M,\nu)}, t\right) = e^{-\lambda t}[\cos(\zeta t) - \cos(st) + \Gamma^{(R)} t\,\mathrm{sinc}(\zeta t)] \tag{8}$$

corresponds to trajectories under sequences of Raman transitions that do not leave the qubit manifold, with effective damped frequency $\zeta = \zeta(J_i^{(M,\nu)}) = \sqrt{s^2(J_i^{(M,\nu)}) - \Gamma^{(0\to1)}\Gamma^{(1\to0)}}$. Equivalent expressions for $I(J_i^{(M,\nu)}, t)$ and $R(J_i^{(M,\nu)}, t)$ were derived previously in Eq. (10) of Ref. [2].

The third term

$$L\left(J_i^{(M,\nu)}, t\right) = \frac{1}{2}\sum_{\alpha=0}^{1} \Gamma^{(\alpha\to g)} f\left(\Gamma^{(\alpha)}, (-1)^\alpha 2J_i^{(M,\nu)}/N, t\right) \tag{9}$$

describes leakage outside the qubit manifold, where $\Gamma^{(0)} = \Gamma^{(0\to g)} + \Gamma^{(1\to g)}$ and $\Gamma^{(1)} = \Gamma^{(1\to g)} + \Gamma^{(1\to0)}$ are the total scattering rates from $|0\rangle$ and $|1\rangle$, respectively, and $f(\Gamma, \chi, t) = e^{i(\chi+i\Gamma)t/2} t\,\mathrm{sinc}[(\chi + i\Gamma)t/2]$.

The final term

$$\begin{aligned} B\left(J_i^{(M,\nu)}, t\right) = {} & \Gamma^{(L)}[a(\lambda, \zeta, t) - a(\lambda, s, t)] + \Gamma^{(B)} b(\lambda, \zeta, t) \\ & + is\Delta^{(L)}[b(\lambda, \zeta, t) - b(\lambda, s, t)] \end{aligned} \tag{10}$$

describes trajectories with both a sequence of Raman transitions and a final leakage transition, with $a(\Gamma, \chi, t) = [f(\Gamma, \chi, t) + f(\Gamma, -\chi, t)]/2$, $b(\Gamma, \chi, t) = -i[f(\Gamma, \chi, t) - f(\Gamma, -\chi, t)]/2\chi$, $\Gamma^{(B)} = (\Gamma^{(0\to1)}\Gamma^{(1\to g)} + \Gamma^{(1\to0)}\Gamma^{(0\to g)})/2$, and $\Delta^{(L)} = (\Gamma^{(0\to g)} - \Gamma^{(1\to g)})/2$.

Metastable qubits in $^{40}Ca^+$. We base our model for photon scattering errors in $^{40}Ca^+$ metastable qubits on the compact Penning trap system operated at GTRI [6]. It exhibits a 0.9 T magnetic field, which splits the neighboring $D_{5/2}$ magnetic sublevels of $^{40}Ca^+$ ions by ∼15 GHz. Off-resonant laser beams with wavelengths near the 854 nm $D_{5/2} \to P_{3/2}$ transition are applied to induce a differential ac Stark shift between two metastable electronic states. As illustrated in Fig. 1(a), we define the qubit states as $|1\rangle \equiv |D_{5/2}, m_J = -5/2\rangle$ and $|0\rangle \equiv |D_{5/2}, m_J = -3/2\rangle$. A linearly polarized infrared laser beam is applied such that only π transitions are coupled, thereby inducing an ac Stark shift on only the $|0\rangle$ state of (in units of s^{-1})

$$\Omega^{(0)} = \frac{6}{5}\frac{A_{P32D52}}{\hbar c k_{DP}^3 \Delta_{P_{3/2}}}\left(\frac{P}{w_0^2}\right), \tag{11}$$

where $\hbar$ is Planck's constant, c is the speed of light, $A_{P32D52} \sim 8.48 \times 10^6$ s^{-1} is the spontaneous decay rate from $P_{3/2}$ to $D_{5/2}$ [19], k_{DP} is the magnitude of the transition k vector, $\Delta_{P_{3/2}} \sim 2\pi \times 1$ THz is the laser beam detuning from resonance, and P (w_0) is the total power (waist) of the shifting laser beam. Scattering rates are [20]

$$\Gamma^{(0\to b)} = A_{P_{3/2}\to b}\left|\frac{\Omega^{(0)}}{\Delta_{P_{3/2}}}\right|, \tag{12}$$

where $A_{P_{3/2}\to b}$ is the spontaneous decay rate from the $P_{3/2}$ sublevel in Fig. 1(a) to a final state b. We find total single-ion scattering rates of <11 s^{-1} for simulations in later sections. When scattering occurs, leakage accounts for 94.5% of the spontaneous decays, while elastic and Raman scattering account for the remaining 1.6% and 3.9%, respectively [19]. Selection rules forbid scattering from $|1\rangle$ under our chosen polarization.

With this setup we generate an effective Hamiltonian $\mathcal{H}_{\mathrm{arm}} = N^{-1}\sum_{i<j} J_{ij} |0_i0_j\rangle \langle 0_i0_j|$ under the light-shift interaction. Ising dynamics (2) are generated by applying $\mathcal{H}_{\mathrm{arm}}$ for time t_{arm} in each of two arms of a spin-echo sequence, yielding terms $|0_i0_j\rangle \langle 0_i0_j| + |1_i1_j\rangle \langle 1_i1_j| = (\sigma_i^z\sigma_j^z + 1)/2$; we treat this spin-echo sequence analytically for the $^{40}Ca^+$ calculations that follow; see SM Sec. C for details [18]. Note that t_{arm} is the relevant scattering timescale and is twice as long as the effective Ising evolution time t. We consider detuning $\delta \equiv \delta_0 \ll \delta_{m\neq0}$ close to the center-of-mass (c.m.) $m = 0$ mode to obtain nearly equal couplings J_{ij}/N and set $t_{\mathrm{arm}} = 2\pi/\delta$ so that the c.m. mode returns to its initial state at the end of each spin-echo arm. We compute the coupling elements J_{ij}/N using zero-temperature simulations of equilibrium ion-crystal configurations as in [21].

GHZ state preparation. As a first application of our model, we examine the preparation of maximally entangled N-ion GHZ or "Schrödinger cat" states [22,23]. An Ising Hamiltonian with uniform coupling J/N produces a GHZ state at the cat time $t_{\mathrm{cat}} = \pi N/4J$

$$|\psi_{\mathrm{GHZ}}\rangle = e^{-iJN^{-1}t_{\mathrm{cat}}\sum_{i<j}\sigma_i^z\sigma_j^z}|+\rangle^{\otimes N} = \frac{|a\rangle^{\otimes N} + e^{i\theta}|b\rangle^{\otimes N}}{\sqrt{2}}, \tag{13}$$

where $|a\rangle \neq |b\rangle$ are eigenstates of σ_i^x for N even or σ_i^y for N odd [13,24]. In practice, the uniformity of the J_{ij} is limited by practical detunings from the c.m. mode; a smaller detuning generates more uniform couplings at the cost of a slower operation.

We use the fidelity $F = \langle\psi_{\mathrm{GHZ}}|\,\rho(t_{\mathrm{cat}})\,|\psi_{\mathrm{GHZ}}\rangle$ to quantify success in GHZ state preparation. Directly calculating F is infeasible at large N because of the exponential size of $\rho(t_{\mathrm{cat}})$, so we estimate F as a product of two parts which are easier to compute.

First, we assume all Ising couplings are equal to their average value $J_{ij} = J$, so ρ can be computed in polynomial time using permutation invariance symmetry [25]. This symmetrized state gives an estimate F_{scatter} for how light scattering affects the fidelity. We calculated the symmetrized state $\rho(t_{\mathrm{cat}})$, and hence F_{scatter}, using our theory; this included the effects of elastic, inelastic, and leakage scattering, and required only minimal computational resources compared to

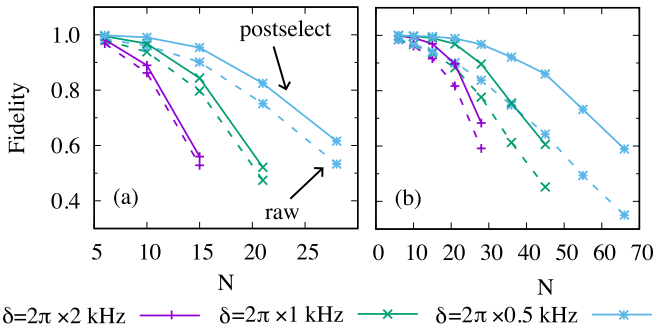

FIG. 2. GHZ state preparation fidelity with (a) $B = 0.9$ T magnetic field and (b) $B = 4.5$ T. Dashed lines are raw results, while solid lines assume postselection to remove leakage.

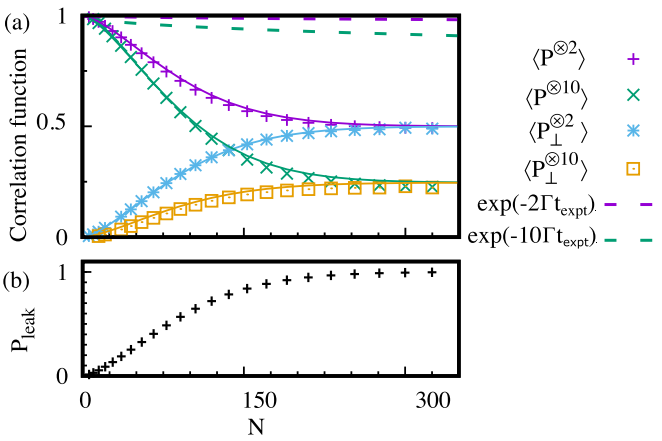

FIG. 3. (a) Spin-spin correlation functions and (b) leakage probability for idealized GHZ state preparation with equal J, with $\delta = 2\pi \times 0.5$ kHz and other parameters from Fig. 2(b). The correlation functions decay from their ideal values much faster than expected from the product of single-ion decoherences (dashed lines). Solid lines are Eqs. (16) and (17).

a direct numerical integration of (4). Second, we use analytic approximations to treat the additional error F_{unequal} due to coupling variations $\delta J_{ij} = J - J_{ij} \neq 0$, which drive ρ away from the ideal GHZ state (13). At second order in the δJ_{ij} and for large N

$$F_{\text{unequal}} \approx \exp\left[-t_{\text{cat}}^2 \sigma^2(J_{ij})/2\right], \tag{14}$$

where $\sigma^2(J_{ij})$ is the variance of the J_{ij}. We evaluate F_{unequal} to fourth order in results that follow; the derivation leading to F_{unequal} is generic and independent of the specific light scattering model (4), with details presented in SM Sec. D [18]. Our total fidelity estimate is $F \approx F_{\text{unequal}} F_{\text{scatter}}$. We will also consider situations in which measurements are used to detect and discard runs with leakage. This improves the scattering fidelity to $F_{\text{scatter}} \approx 1$, with small residual error due to elastic and Raman scattering.

Figure 2(a) shows our estimated F for GHZ states prepared in a 0.9 T magnetic field. Each curve terminates when larger sizes would result in $F < 0.5$. The dashed lines illustrate the raw F, while solid lines illustrate $F_{\text{postselect}}$ after postselection is used to remove leakage. Postselection yields a notable improvement, though $F_{\text{postselect}} \approx F_{\text{unequal}}$ is ultimately limited by the use of unequal couplings J_{ij}.

Postselection requires an expected sampling overhead $1/P_{\text{no leak}}$, where $P_{\text{no leak}}$ is the probability of no leakage. We can compute this from the fidelities in Fig. 2 by considering that the raw F is an average over trajectories with and without leakage, $F = P_{\text{no leak}} F_{\text{no leak}} + P_{\text{leak}} F_{\text{leak}} = P_{\text{no leak}} F_{\text{no leak}}$, where the last equality uses $F_{\text{leak}} = 0$ since the GHZ state has zero overlap with the ground-state subspace. After postselection the fidelity improves to $F = F_{\text{no leak}}$. Hence the expected sampling overhead $1/P_{\text{no leak}} = F_{\text{postselect}}/F$ and this is close to one for the results in Fig. 2(a).

To understand prospects for GHZ preparation at larger sizes, in Fig. 2(b) we increase the strength of the magnetic field to 4.5 T, which spreads the vibrational mode spectrum to decrease the variance $\sigma^2(J_{ij})$. We estimate that GHZ states can be produced at approximately twice the sizes seen previously in Fig. 2(a), with greater gains from postselection. Another approach to reducing the spread in J_{ij} could be to engineer a more uniform coupling using a multitone optical dipole force that simultaneously drives all axial motional modes [26]. Alternately, dispersive measurements have been proposed as a nondeterministic means to generate large GHZ states with high fidelity [27].

Correlation functions. Quantum simulations often rely on "local" or few-body observables, which may be much less sensitive to noise than the global state fidelity. Here we quantify the accuracy of m-body spin-spin correlation functions. GHZ states (13) constitute ideal standards for this analysis, since GHZ states polarized along $P \in \{\sigma^x, \sigma^y\}$ will satisfy $\langle P^{\otimes 2m} \rangle = 1$ for any even number of ions $2m$. To compare against this standard we analyze spin correlation functions assuming an equal coupling $J_{ij} = J$, so that any deviation $\langle P^{\otimes 2m} \rangle \neq 1$ is attributable directly to light-scattering errors. We expect similar physics in other cases, such as GHZ state preparation with unequal J_{ij} and quantum simulations with strong couplings, with the additional complication that the noiseless reference $\langle P^{\otimes 2m} \rangle \neq 1$ will depend on details of the J_{ij} and may therefore be much more variable.

Figure 3(a) shows two-body and ten-body spin-spin correlation functions. There are significant deviations away from the ideal value $\langle P^{\otimes 2m} \rangle = 1$, which exceed the decay $\exp(-2m\Gamma t_{\text{expt}})$ arising from the product of $2m$ single-ion decoherences (dotted lines), where $t_{\text{expt}} = 2t_{\text{arm}}$ is the total length of the simulated experiment. The simple model below will attribute the additional error to dynamical interactions with leaked qubits; the probability for at least one qubit to leak is shown in Fig. 3(b).

If an ion leaks to $|g\rangle$, it generates an effective magnetic field $\exp[-i(\theta/2)\sum_{i \neq l} \sigma_i^z]$, where $\theta/2 \leqslant Jt_{\text{cat}}/N = \pi/4$ for GHZ state preparation. In addition to this field, the remaining ions evolve under $\exp[-i(\pi/4)\sum_{i<j}^{N-1} \sigma_i^z \sigma_j^z]$, which alone would generate an $(N-1)$-ion GHZ state that is polarized in the spin direction $P_\perp$ perpendicular to the N-ion GHZ spin direction P [where $P = \sigma^x$ when N is even and $P = \sigma^y$ when N is odd; see (13)]. The effective magnetic field rotates the polarization phase θ of the $(N-1)$-ion GHZ state to $P_\theta = \cos(\theta) P_\perp \pm \sin(\theta) P$. In summary, single-ion leakage produces an $(N-1)$-ion GHZ state with a random phase,

depending on the leakage time. Multiple-ion leakage produces a smaller, but similarly randomized GHZ state.

Approximating the probability distribution over angles as uniform, we expect the projection along the intended spin orientation P in the presence of leakage to be

$$\langle P^{\otimes 2m}\rangle_{\text{leak}} \approx \frac{2}{\pi}\int_0^{\pi/2} d\theta\, \langle\psi_{\text{GHZ}}|\, P_\theta^{\otimes 2m}\,|\psi_{\text{GHZ}}\rangle = \frac{2}{\pi}\int_0^{\pi/2} d\theta\, \sin^{2m}(\theta) = \frac{1}{\sqrt{\pi}}\frac{\Gamma\left(\frac{1}{2}+m\right)}{\Gamma(1+m)}, \quad (15)$$

where the Γ are Gamma functions. Using similar reasoning we obtain the same result for the perpendicular direction, $\langle P_\perp^{\otimes 2m}\rangle_{\text{leak}} = \langle P^{\otimes 2m}\rangle_{\text{leak}}$.

We are now ready to estimate the $\langle P^{\otimes 2m}\rangle$ as a sum of parts with and without leakage, neglecting small errors from elastic and Raman scattering to simplify our reasoning. In this approximation, the probability of ideal evolution is $P_{\text{no leak}} = \exp(-N\Gamma^{(0\to g)}t_{\text{arm}})$, with spin-correlation $\langle P^{\otimes 2m}\rangle_{\text{no leak}} = 1$, while the probability for leaky evolution is $P_{\text{leak}} = 1 - P_{\text{no leak}}$, with spin-correlation $\langle P^{\otimes 2m}\rangle_{\text{leak}}$. Then in total we expect

$$\langle P^{\otimes 2m}\rangle \approx e^{-N\Gamma^{(0\to g)}t_{\text{arm}}} + \frac{\left(1-e^{-N\Gamma^{(0\to g)}t_{\text{arm}}}\right)\Gamma\left(\frac{1}{2}+m\right)}{\sqrt{\pi}\Gamma(1+m)}. \quad (16)$$

We also expect that the perpendicular direction will have a nonzero correlation due solely to leakage

$$\langle P_\perp^{\otimes 2m}\rangle \approx \frac{\left(1-e^{-N\Gamma^{(0\to g)}t_{\text{arm}}}\right)\Gamma\left(\frac{1}{2}+m\right)}{\sqrt{\pi}\Gamma(1+m)}. \quad (17)$$

The simple model (16),(17) corresponds to the solid curves in Fig. 3(a). It accounts for the majority of the observed error in the exact results (data points) computed from relations equivalent to (6)–(10) but also including an analytic treatment of a spin echo for $^{40}Ca^+$, as mentioned earlier and described in SM Sec. C [18]. To correct this error, postselection can be used to discard runs with leakage, with an expected sampling overhead of $1/(1-P_{\text{leak}})$. Repeated spin-echo sequences could mitigate the errors through partial cancellations.

Spin squeezing. Quantum metrology seeks to enhance sensing capabilities using quantum entanglement in protocols such as spin squeezing [3,14,28–30]. Squeezing decreases the collective spin variance along a chosen axis to enhance sensitivity, as quantified by the spin squeezing parameter

$$\xi_R^2 = \min_\theta \frac{N(\Delta S^\theta)^2}{|\langle S^x\rangle|^2}, \quad (18)$$

where $S^x = (1/2)\sum_i \sigma_i^x$ and $S^\theta = (1/2)\sum_i \cos(\theta)\sigma_i^z + \sin(\theta)\sigma_i^y$ are collective spin vectors. In the unentangled initial state, $\xi_R^2 = 1$. The Ising evolution (2) squeezes the state through approximate "one-axis twisting" leading to $\xi_R^2 < 1$ [14].

Figure 4 shows ξ_R^2 for a variety of sizes, with detuning $\delta = 2\pi \times 2$ kHz, $B = 0.9$ T, and with the exact J_{ij} for $^{40}Ca^+$. In these results we minimized ξ_R^2 at each N by varying the average coupling strengths J/N; best-fit results follow $Jt/N \approx 0.85N^{-0.62} \ll 1$ as shown in SM Sec. E [18], which corresponds to a much weaker coupling than the one employed in GHZ state preparation (recall for GHZ states, $Jt_{\text{cat}}/N = \pi/4$). We find that scattering causes only minor errors in ξ_R^2 relative

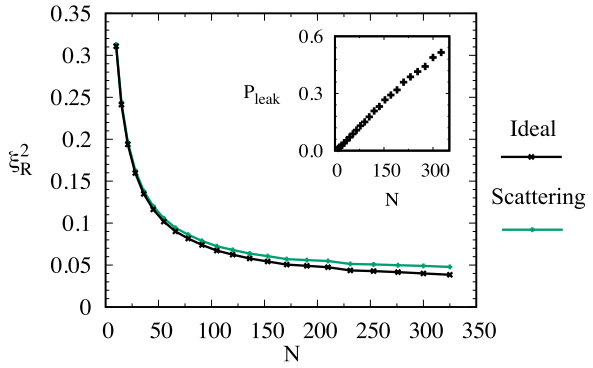

FIG. 4. Optimal spin squeezing parameter ξ_R^2 with and without light scattering errors. Inset: leakage probability.

to the ideal case, even with a few hundred ions where leakage is likely (Fig. 4 inset).

We attribute the error resilience of spin squeezing to weak coupling. If an ion leaks to its ground state, then it generates an effective magnetic field $\exp(-iN^{-1}\sum_i J_{il}t_l\sigma_i^z)$, where t_l is the time of leakage, but for weak coupling $Jt/N \ll 1$ this field is close to the identity and does not contribute to significant error. Apart from this effective field, the ions also evolve under the $(N-1)$-ion version of $\mathcal{H}$, which leads to a ξ_R^2 similar to the case without leakage. We find similar results for a simple benchmarking implementation of single-layer QAOA in SM Sec. E [18].

Conclusions. We analytically solved a model of metastable-qubit Ising dynamics in the presence of light scattering errors, including inelastic, elastic, and leakage scattering channels, as pictured in Fig. 1(b). These analytic results allow for modeling of experiments with large numbers of ions N, where numerical simulation of the quantum state is prohibitively difficult or impossible.

Our main findings with respect to the physical effect of leakage are as follows. (1) When a qubit leaks outside the qubit manifold, then its Ising interaction with the other qubits behaves as an "effective magnetic field" that is applied up until the leakage event occurs. The strength of the field depends on the coupling strength and on the specific leakage time, the latter of which is random. The physical effect of these fields is that all nonleaked qubits will rotate between the Pauli spin directions σ^x and σ^y. (2) Depending on the coupling-time product Jt/N that is present in a given experiment, the effective magnetic fields that are generated in leakage may have catastrophic or negligible effects. When $Jt/N \approx 1$, as in GHZ state preparation or strongly coupled quantum simulations, then the effective magnetic fields completely randomize the Pauli spin directions σ^x and σ^y for all nonleaked qubits. When leakage occurs, these errors must be addressed to obtain accurate results, for example, by postselecting on the presence of even a single leaked qubit. When $Jt/N \ll 1$, as in spin squeezing, then the nonleaked qubits rotate by only a negligible angle under the effective magnetic fields. Therefore, in this case leakage does not significantly affect accuracy.

In conclusion, we have developed analytic theory that quantifies and provides physical insights into leakage errors in trapped-ion quantum simulations. In this context, observables

in a given experiment can be readily computed using the relevant Ising couplings, scattering rates, and experimental run times. We expect our results to be useful in estimating experimental tradeoffs obtained for different choices of experimental parameters, such as coupling strengths and sampling overheads for postselection, as well as modeling a variety of future experiments.

Code verifying the correctness of the analytical results is available at [31].

Acknowledgments. The authors would like to thank J. Bollinger, J. Wang, B. Gard, and R. Bennink for providing useful comments on this manuscript. This material is based upon work supported by the Defense Advanced Research Projects Agency (DARPA) under Contract No. HR001120C0046. This work has been partially supported by U.S. DOE. ORNL is managed by UT-Battelle, LLC, under Contract No. DE-AC0500OR22725 with the U.S. Department of Energy. The U.S. Government retains and the publisher, by accepting the article for publication, acknowledges that the U.S. Government retains a nonexclusive, paid-up, irrevocable, worldwide license to publish or reproduce the published form of this manuscript, or allow others to do so, for the U.S. Government purposes. The Department of Energy will provide public access to these results of federally sponsored research in accordance with the DOE Public Access Plan.

[1] D. T. C. Allcock, W. C. Campbell, J. Chiaverini, I. L. Chuang, E. R. Hudson, I. D. Moore, A. Ransford, C. Roman, J. M. Sage, and D. J. Wineland, *omg* blueprint for trapped ion quantum computing with metastable states, Appl. Phys. Lett. **119**, 214002 (2021).

[2] M. Foss-Feig, K. R. A. Hazzard, J. J. Bollinger, and A. M. Rey, Nonequilibrium dynamics of arbitrary-range Ising models with decoherence: An exact analytic solution, Phys. Rev. A **87**, 042101 (2013).

[3] J. G. Bohnet, B. C. Sawyer, J. W. Britton, M. L. Wall, A. M. Rey, M. Foss-Feig, and J. J. Bollinger, Quantum spin dynamics and entanglement generation with hundreds of trapped ions, Science **352**, 1297 (2016).

[4] M. Gärttner, J. G. Bohnet, A. Safavi-Naini, M. L. Wall, J. J. Bollinger, and A. M. Rey, Measuring out-of-time-order correlations and multiple quantum spectra in a trapped-ion quantum magnet, Nat. Phys. **13**, 781 (2017).

[5] K. A. Gilmore, M. Affolter, R. J. Lewis-Swan, D. Barberena, E. Jordan, A. M. Rey, and J. J. Bollinger, Quantum-enhanced sensing of displacements and electric fields with two-dimensional trapped-ion crystals, Science **373**, 673 (2021).

[6] B. J. McMahon, K. R. Brown, C. D. Herold, and B. C. Sawyer, Individual-ion addressing and readout in a Penning trap, arXiv:2404.02105.

[7] Y. Wu, S. Kolkowitz, S. Puri, and J. D. Thompson, Erasure conversion for fault-tolerant quantum computing in alkaline earth Rydberg atom arrays, Nat. Commun. **13**, 4657 (2022).

[8] M. Kang, W. C. Campbell, and K. R. Brown, Quantum error correction with metastable states of trapped ions using erasure conversion, PRX Quantum **4**, 020358 (2023).

[9] B. C. Sawyer and K. R. Brown, Wavelength-insensitive, multispecies entangling gate for group-2 atomic ions, Phys. Rev. A **103**, 022427 (2021).

[10] C. Monroe, W. C. Campbell, L.-M. Duan, Z.-X. Gong, A. V. Gorshkov, P. W. Hess, R. Islam, K. Kim, N. M. Linke, G. Pagano *et al.*, Programmable quantum simulations of spin systems with trapped ions, Rev. Mod. Phys. **93**, 025001 (2021).

[11] H. Uys, M. J. Biercuk, A. P. Van Devender, C. Ospelkaus, D. Meiser, R. Ozeri, and J. J. Bollinger, Decoherence due to elastic Rayleigh scattering, Phys. Rev. Lett. **105**, 200401 (2010).

[12] M. Foss-Feig, Quantum simulation of many-body physics with neutral atoms, molecules, and ions, Ph.D. thesis, University of Colorado Boulder, 2012.

[13] D. Leibfried, E. Knill, S. Seidelin, J. Britton, R. B. Blakestad, J. Chiaverini, D. B Hume, W. M. Itano, J. D. Jost, C. Langer *et al.*, Creation of a six-atom 'Schrödinger cat' state, Nature (London) **438**, 639 (2005).

[14] L. Pezze, A. Smerzi, M. K. Oberthaler, R. Schmied, and P. Treutlein, Quantum metrology with nonclassical states of atomic ensembles, Rev. Mod. Phys. **90**, 035005 (2018).

[15] J. Rajakumar, J. Moondra, B. Gard, S. Gupta, and C. D. Herold, Generating target graph couplings for the quantum approximate optimization algorithm from native quantum hardware couplings, Phys. Rev. A **106**, 022606 (2022).

[16] H. Carmichael, *An Open Systems Approach to Quantum Optics: Lectures Presented at the Université Libre de Bruxelles, October 28 to November 4, 1991* (Springer Science & Business Media, New York, 2009), Vol. 18.

[17] W. H. Press, B. P. Flannery, and S. A. Teukolsky, *Numerical Recipes in Fortran 77: The Art of Scientific Computing*, 2nd ed. (Cambridge University Press, Cambridge, UK, 1996).

[18] See Supplemental Material at http://link.aps.org/supplemental/10.1103/PhysRevA.110.L030803 for technical derivations and additional details of the experimental modeling.

[19] R. Gerritsma, G. Kirchmair, F. Zähringer, J. Benhelm, R. Blatt, and C. F. Roos, Precision measurement of the branching fractions of the $4p^2 2P_{3/2}$ decay of Ca II, Eur. Phys. J. D **50**, 13 (2008).

[20] D. J. Wineland, M. Barrett, J. Britton, J. Chiaverini, B. DeMarco, W. M. Itano, B. Jelenkovic, C. Langer, D. Leibfried, V. Meyer, T. Rosenband, and T. Schatz, Quantum information processing with trapped ions, Philos. Trans. R. Soc. A **361**, 1349 (2003).

[21] C.-C. J. Wang, A. C. Keith, and J. K. Freericks, Phonon-mediated quantum spin simulator employing a planar ionic crystal in a Penning trap, Phys. Rev. A **87**, 013422 (2013).

[22] D. M. Greenberger, M. A. Horne, and A. Zeilinger, Going beyond Bell's theorem, *Bell's Theorem, Quantum Theory and Conceptions of the Universe* (Springer, Berlin, 1989), pp. 69–72.

[23] N. D. Mermin, Extreme quantum entanglement in a superposition of macroscopically distinct states, Phys. Rev. Lett. **65**, 1838 (1990).

[24] K. Mølmer and A. Sørensen, Multiparticle entanglement of hot trapped ions, Phys. Rev. Lett. **82**, 1835 (1999).

[25] M. Gegg and M. Richter, Efficient and exact numerical approach for many multi-level systems in open system CQED, New J. Phys. **18**, 043037 (2016).

[26] Y. Shapira, R. Shaniv, T. Manovitz, N. Akerman, L. Peleg, L. Gazit, R. Ozeri, and A. Stern, Theory of robust multiqubit

nonadiabatic gates for trapped ions, Phys. Rev. A **101**, 032330 (2020).

[27] B. Alexander, J. J. Bollinger, and H. Uys, Generating Greenberger-Horne-Zeilinger states with squeezing and postselection, Phys. Rev. A **101**, 062303 (2020).

[28] D. J. Wineland, J. J. Bollinger, W. M. Itano, F. L. Moore, and D. J. Heinzen, Spin squeezing and reduced quantum noise in spectroscopy, Phys. Rev. A **46**, R6797 (1992).

[29] M. Kitagawa and M. Ueda, Squeezed spin states, Phys. Rev. A **47**, 5138 (1993).

[30] D. J. Wineland, J. J. Bollinger, W. M. Itano, and D. J. Heinzen, Squeezed atomic states and projection noise in spectroscopy, Phys. Rev. A **50**, 67 (1994).

[31] https://code.ornl.gov/5ci/exactly-solved-model-of-light-scattering-errors-in-quantum-simulations-with-metastable-trapped-ion-qubits